EPFL peptide signaling ensures robust self-pollination success under cool temperature stress by aligning the length of the stamen and pistil

Satomi Negoro[1], Tomo Hirabayashi[2], Rie Iwasaki[2], Keiko U. Torii[2,3], and Naoyuki Uchida[1,2]

[1]Center for Gene Research, Nagoya University, Nagoya 464-8602, Japan

[2]Institute of Transformative Bio-Molecules, Nagoya University, Furo-cho, Chikusa-ku, Nagoya, 464-8601, Japan

[3]Department of Molecular Biosciences and Howard Hughes Medical Institute, The University of Texas at Austin, 2506 Speedway, Austin, TX 78712, USA

Author for correspondence:

Naoyuki Uchida

Tel: +81-52-789-3080

E-mail: uchinao@gene.nagoya-u.ac.jp

Summary Statement:

The secretory peptide EPFL6 promotes stamen elongation to ensure robust self-pollination under cool temperature stress in *Arabidopsis thaliana*. On the other hand, its receptor ERECTA contributes to self-pollination by aligning the lengths of stamen and pistils at moderate and cool temperatures.

Abstract

Successful sexual reproduction of plants requires temperature-sensitive processes, and temperature stress sometimes causes developmental asynchrony between male and female reproductive tissues. In *Arabidopsis thaliana,* self-pollination occurs when the stamen and pistil lengths are aligned in a single flower so that pollens at the stamen tip are delivered to the stigma at the pistil tip. Although intercellular signaling acts in several reproduction steps, how signaling molecules, including secreted peptides, contribute to the synchronous growth of reproductive tissues remains limited. Here we show that the mutant of the secreted peptide *EPIDERMAL PATTERNING FACTOR LIKE 6* (*EPFL6*), which shows no phenotypes at a moderate temperature, fails in fruit production at a cool temperature due to insufficient elongation of stamens. *EPFL6* is expressed in stamen filaments and promotes filament elongation to achieve the alignment of stamen and pistil lengths at a cool temperature. We also found that, at a moderate temperature, all *EPFL6*-subfamily genes are required for stamen elongation. Furthermore, we showed that ERECTA (ER), known as a common receptor for EPFL-family peptides, mediates the stamen-pistil growth coordination. Lastly, we provided evidence that modulation of ER activity rescues the reproduction failure caused by insufficient stamen elongation through realigning the stamen and pistil lengths.

Key words:

Arabidopsis thaliana; EPFL; ERECTA; Temperature; Pistil; Self-pollination; Stamen; Reproduction

Introduction

Most flowering plant species require pollination for successful reproduction. Pollination is classified into two forms: self-pollination and cross-pollination (Fattorini & Glover, 2020). Self-pollination has the advantage of leaving offspring more easily than cross-pollination, while it leads to a decrease in the genetic diversity of offspring. On the other hand, cross-pollination contributes to an increase in genetic diversity, while it requires pollinators for reproductive success. Self-pollination occurs when the stamen and pistil mature at the same time in a single flower, and pollens from the stamen can be delivered to the stigma at the tip of the pistil. Some species have evolved physical features of floral organs to prevent self-pollination (Barrett, 2002; Kappel et al., 2017). For example, in distylous primroses, each individual develops one of two flower types with differences in stamen and pistil length, a flower with a long pistil and short stamens or one with a short pistil and long stamens. These morphological features serve as barriers to self-pollination. Conversions between self- and cross-pollination have occurred multiple times within the angiosperms in evolution (Barrett, 2002). It is also known that environmental changes sometimes induce temporal pollination-type conversions (Kalisz & Vogler, 2003; Kalisz et al., 2004). In environments where pollinator activities are compromised, a shift from cross-pollination to self-pollination provides reproductive assurance (Kumar et al., 2019). Conversely, for self-pollinating species, conditional self-pollination failure due to insufficient growth of either male or female tissues caused by environmental changes such as low-temperature stress can prompt occasional cross-pollination, resulting in an increase in genetic diversity (Liu et al., 2019). Nevertheless, in general, robust self-pollination success against environmental stress is critical to stable propagation for self-pollinating species.

Environmental fluctuations can be detrimental to reproduction, and temperature fluctuation is a major unavoidable stress in natural environments (Gray & Brady, 2016; Haider et al., 2021; Lamers et al., 2020). Successful sexual reproduction requires a series of

68 temperature-sensitive processes (Liu et al., 2019; Lohani et al., 2020; Zinn et al., 2010), and
69 temperature fluctuation sometimes causes asynchrony between male and female reproductive
70 development (Hedhly et al., 2009; Herrero, 2003). Therefore plants have evolved
71 developmental programs with robust tolerance to temperature fluctuation for reproductive
72 success (Casal & Balasubramanian, 2019; Ding et al., 2020). In particular, for self-pollinating
73 species, mechanisms ensuring the robust synchronous growth of the stamen and pistil in a single
74 flower are critically important to assure reproductive success.

75 The *Arabidopsis thaliana* genome retains eleven *EPIDERMAL PATTERNING*
76 *FACTOR LIKE* (*EPFL*) genes encoding a family of plant-specific cysteine-rich secreted
77 peptides, several of which were reported to act as developmental regulators (Tameshige et al.,
78 2017). *EPFL*-family genes are conserved in land plant species, and the common structure of
79 EPFL peptides is a relatively conserved scaffold domain and a variable loop domain (Takata et
80 al., 2013). The EPFL peptides are classified into five subfamilies based on their amino-acid
81 sequences (Rychel et al., 2010; Takata et al., 2013). EPF1, EPF2, and EPFL7 belong to the
82 same subfamily, which is closely related to another subfamily including EPFL9/STOMAGEN.
83 Other subfamilies are one consisting of EPFL1, EPFL2, and EPFL3, and the other including
84 EPFL4/CHALLAH-LIKE1, EPFL5/CHALLAH-LIKE2, and EPFL6/CHALLAH. EPFL8
85 seems to constitute an additional subfamily (Bessho-Uehara et al., 2016). EPF1, EPF2, and
86 EPFL9 control stomatal patterning (Hara et al., 2007; Hara et al., 2009; Hunt et al., 2010; Hunt
87 & Gray, 2009; Kondo et al., 2010; Lee et al., 2015; Lee et al., 2012; Sugano et al., 2010). EPFL4
88 and EPFL6 promote the growth of inflorescence stems (Abrash et al., 2011; Uchida et al., 2012;
89 Uchida & Tasaka, 2013). EPFL2 enhances the outgrowth of leaf serration (Tameshige et al.,
90 2016). EPFL2 also coordinates the arrangement of ovules in pistils with EPFL9 (Kawamoto et
91 al., 2020). Furthermore, EPFL1, EPFL2, EPFL4, and EPFL6 coordinately regulate the
92 morphology of the shoot apical meristem (Kosentka et al., 2019).

EPFL4 and EPFL6 peptides act as redundant ligands for their receptor protein called ERECTA (ER) (Abrash et al., 2011; Uchida et al., 2012), which has been shown as a common receptor for several EPFL-family peptides (Lee et al., 2012; Tameshige et al., 2016; Uchida et al., 2012). Although neither *epfl4* nor *epfl6* single mutants show any obvious phenotypes, *epfl4 epfl6* double mutant (hereafter *epfl4/6*) develops shorter internodes between siliques than wild-type plants. It is unknown whether either or both of *EPFL4*/*6* genes have a role in developmental robustness against environmental fluctuation. This study shows that *EPFL6* prevents insufficient elongation of stamens under low-temperature stress to ensure robust alignment of stamen and pistil lengths. We also found that, at a moderate temperature, all genes of the *EPFL6*-including subfamily are required for the proper stamen-pistil growth coordination. Furthermore, we revealed that the receptor ER regulates the alignment of stamen and pistil lengths. Lastly, we provided evidence that modulation of the ER signaling can be utilized to rescue the reproduction failure caused by insufficient elongation of stamens through realigning the stamen and pistil lengths.

Materials and Methods

Plant materials and growth conditions

The *Arabidopsis thaliana* accession Columbia-0 was used as the wild type in this study. *epfl4* (Salk_071065), *epfl5* (Salk_005080), *epfl6* (Salk_072522), *myb21* (Salk_042711), *er-105*, *EPFL4pro:GUS*, *EPFL5pro:GUS*, *EPFL6pro:GUS*, *ERpro:GUS, SUC2pro:ER* and *ERpro:ER-YFP* were described previously (Ikematsu et al., 2017; Mandaokar et al., 2006; Shpak et al., 2004; Torii et al., 1996; Uchida et al., 2012; Uchida & Tasaka, 2013). Plant seeds were sterilized, plated on 0.5 x Murashige and Skoog medium, stored in the dark at 4 °C for at

least two days, and grown at 22 °C under continuous light. Seedlings are transplanted and grown on soil at 16 °C or 22 °C under continuous light. After inflorescence stems emerged, plants were grown in an environment where special care was taken to ensure that air currents and vibrations did not shake stems and cause unexpected dispersal of pollens in developing flowers. Anti-vibration rubber sheets were placed under growth shelves to reduce vibrations. When *epfl4/5/6* or *myb21* homozygous seeds were needed, the mutant stems were shaken by hand once a day, which forced self-pollination by artificially scattering pollens inside flowers.

Plasmid construction and generation of transgenic plants

Plasmids constructed in this study and primers used for the plasmid construction are listed in Tables S1 and S2, respectively. *Agrobacterium tumefaciens* strain GV3101 was used for plant transformation via the floral dip method (Clough & Bent, 1998). *SCARECROW* (*SCR*) *pro:GUS* and *INDOLE-3-ACETIC ACID INDUCIBLE 19* (*IAA19*) *pro:GUS* were introduced into Col, and *EPFL6pro:EPFL6*, *SCRpro:EPFL6*, *IAA19pro:EPFL6* were introduced into *epfl6*. More than fifteen T1 plants were generated for each construct, and at least two lines harboring the corresponding transgene at a single locus were selected for further analyses.

Measurement of stamen and pistil lengths

Flowers at various developmental stages were collected from plants grown in multiple batches to broadly cover each graph's x-axis range. Sepals and petals were removed with forceps under a stereomicroscope (Zeiss, Stemi2000CS) to observe each flower's stamens and pistil. Images of the dissected samples were taken with a color camera (Zeiss, Axiocam HRc). Lengths of the pistil (from the pistil base to just below the stigma) and the longest stamen (from the filament base to just below the anther) in each flower image were measured using ImageJ (Schneider et al., 2012).

143

144 **Measurement of the length and number of epidermal cells of filaments**

145 Entire flowers were cleared with a chloral hydrate-based clearing solution (8 g chloral hydrate,
146 1 ml glycerol, and 2 ml water). Stamens were isolated with forceps under a stereomicroscope
147 (Zeiss, Stemi2000CS). Differential interference contrast (DIC) images of the cleared stamens
148 were taken using an upright microscope (Zeiss, Axio Imager.A2) and a color camera (Zeiss,
149 Axiocam 512 color). The DIC images from each stamen were stitched to make a full-length
150 image of the filament, and cell length along the long axis of the filament was measured using
151 ImageJ. The filament epidermis consists of aligned cell files (See the explanation of "cell file"
152 in the Result section), and the number of cells included in each cell file was counted using the
153 stitched images.

154

155 **qRT-PCR**

156 Each RNA sample was prepared from a pool of 42 filaments after the removal of anthers. Total
157 RNAs were extracted and purified using RNeasy Plant Mini Kit (QIAGEN). Three independent
158 RNA samples under each condition were used for quantitative reverse transcription PCR (qRT-
159 PCR). Reverse transcription was carried out using ReverTra Ace (TOYOBO). Quantitative
160 PCR (qPCR) was performed using SYBER FAST qPCR Kit (KAPA) and LightCycler 96
161 (Roche). The primers used for qPCR are listed in Table S2.

162

163 **GUS staining**

164 GUS staining was performed as described previously (Uchida et al., 2011). After inflorescences
165 with flowers were GUS-stained, the samples were cleared with a chloral hydrate-based clearing
166 solution. Sepals and petals were removed from the cleared flowers with forceps to observe each

flower's stamens and pistil. Images were taken using a stereomicroscope (Zeiss, Stemi2000CS) and a color camera (Zeiss, Axiocam HRc).

Confocal microscopy

Samples for confocal microscopy observation were prepared by the ClearSee method for deep imaging (Kurihara et al., 2015). Inflorescence tips with flowers were fixed in 4% (w/v) PFA supplemented with 0.1% Triton X-100, preventing samples from repelling the fixing solution. After the samples were cleared, filaments were prepared by removing sepals and petals with forceps under a stereomicroscope (Zeiss, Stemi2000CS). YFP and tdTomato fluorescence was observed by confocal microscopy (Zeiss, LSM900) with excitation at 488 nm and 561 nm, respectively. Detection ranges were 500-550 nm for YFP and 565-700 nm for tdTomato. DIC images were taken by a T-PMT detector.

Results

Reproductive success at a cool temperature requires the secreted peptide EPFL6.

In the process of analyzing the defect of internode elongation in *epfl4/6* double mutant, we unexpectedly found that *epfl4/6* did not develop functional siliques when grown at a lower temperature (16 °C) than a moderate temperature (22 °C), only forming pedicels with undeveloped siliques (Fig. 1a). Such a reproduction failure has never been observed at 22 °C. To examine whether simultaneous loss of *EPFL4* and *EPFL6* is required to cause the reproduction failure phenotype, each single mutant was grown at 16 °C. As a result, *epfl4* developed functional siliques, while *epfl6* did not, indicating that a loss of function of a single gene, *EPFL6,* causes the reproduction failure at 16 °C, which is in sharp contrast to the

observation that *epfl6* formed functional silique at 22 °C (Fig. S1a). These results provided the first evidence that *EPFL6* is required for reproductive success at a low temperature.

EPFL6 promotes stamen growth to align the length of stamens and a pistil in a single flower for successful self-pollination at a cool temperature.

To investigate how the *epfl6* mutation causes the reproduction failure, we examined whether pollination occurs in *epfl6* flowers at 16 °C (Fig. 1b). An *Arabidopsis thaliana* flower develops four long stamens and two short ones (Bowman, 1994). In wild-type plants, when lengths of long stamens and a pistil became almost equal in a single flower, anthers at the tips of the stamens were able to deliver pollen grains to the stigma at the tip of the pistil, providing a suitable situation for self-pollination success (Fig. 1b). Each dot in scatter plots in Fig. 1c,d shows the relation of the lengths of the pistil and the longest stamen in a single flower at various developing stages at 22 °C or 16 °C. If the stamen length is nearly equal to the pistil length, such dots are located on or close to the diagonal line in each plot, showing a high expectation of successful pollination. In wild-type flowers, although stamens were shorter than a pistil in the early phase of flower development, stamens eventually elongated enough to catch up with the pistil growth in the later phase. On the other hand, in *epfl6* flowers, in contrast to stamens grown at 22 °C (Fig. S1b) that elongated as long as pistils to achieve successful self-pollination, stamens at 16 °C did not elongate long enough for anthers to touch the stigma (Fig. 1b-d). Compared with wild-type stigma covered with a substantial number of pollens, pollens in *epfl6* flowers at 16 °C were attached only to the side surface of the pistil distantly apart from the stigma (Fig. 1b, arrows). Pollen attachment to the stigma was observed in *epfl4* flowers but not in *epfl4/6* flowers at 16 °C (Fig. 1b), consistent with their silique phenotypes (Fig. 1a). Next, the functionality of *epfl6* mutant pollens was examined by a hand-pollination experiment using the pistil and stamens of *epfl6* flowers. When *epfl6* pollens were hand-pollinated to the stigma

of the same flower (Fig. S1c), the treated pistil developed a normal silique with viable seeds. These results show that the reproduction failure of *epfl6* at a low temperature is caused by failure of pollen delivery to the stigma, not by the dysfunctionality of pollens or stigma.

EPFL6 promotes cell proliferation of stamen filaments at a cool temperature.

Stamen elongation is attributed to the proliferation and elongation of cells that constitute a stamen filament. To unravel the underlying cellular defects of *epfl6* short stamens at 16 °C, we compared the length and number of epidermal cells of filaments between wild-type and *epfl6* stamens. We selected flowers with an about 2.5-mm pistil for this analysis since such flowers were at the developmental stage suitable for self-pollination in the wild type (Fig. 1b,d). Although the length of epidermal cells varied to some extent, the average length was similar between wild-type and *epfl6* (Fig. 2a,b). In the filament epidermis, cells were orderly arranged in a vertical direction, which we defined as "cell file", and the filament epidermis was composed of aligned cell files (Fig. 2a; an example of "cell file" was shown by dots, where each dot marks an individual cell in a representative file). The number of cells from the bottom end to the top end in each cell file was noticeably less in *epfl6* than in wild type (Fig. 2c). Together, the reduction in the number of filament cells, not cell length, accounts for short stamens in *epfl6.* Thus, *EPFL6* ensures the robust proliferation of filament cells against low-temperature stress.

EPFL6 expression in filaments is sufficient for self-pollination success at a cool temperature.

Previous studies reported that *EPFL6* is expressed in inflorescence stems to promote stem growth (Abrash et al., 2011; Uchida et al., 2012), while its expression in stamens has not been described. To investigate the *EPFL6* expression in reproductive tissues, we analyzed *EPFL6pro:GUS* plants with the *EPFL6* promoter fragment that rescued the reproduction failure

of *epfl6* at 16 °C when fused with the *EPFL6* coding sequence (Fig. 3b). The *EPFL6* promoter activity was detected in stamen filaments and anthers in addition to inflorescence stems (Fig. 3a). It was reported that the *EPFL6* expression driven by the *SCARECROW* (*SCR*) promoter, which is active in endodermal cells of inflorescence stems, rescues the short internode phenotype of the *epfl4/6* stem (Uchida et al., 2012). However, unlike in inflorescence stems, *SCRpro:GUS* signals were not detected in stamens (Fig. 3c). The *SCRpro:EPFL6* did not rescue the reproduction failure of *epfl6* at 16 °C (Fig. 3d), showing that the *EPFL6* expression in stems does not contribute to the rescue. In contrast, when *EPFL6* was expressed by the *INDOLE-3-ACETIC ACID INDUCIBLE 19* (*IAA19*) promoter that was active in stamen filaments but not in stems and anthers (Fig. 3e), the *IAA19pro:EPFL6* rescued the reproduction failure of *epfl6* at 16 °C (Fig. 3f). These results demonstrate that the *EPFL6* expression in filaments contributes to reproduction success at a low temperature. Comparison of expression levels of *EPFL6* in filaments between 22 °C and 16 °C by quantitative reverse transcription PCR (qRT-PCR) showed that the *EPFL6* expression level is not significantly changed by low-temperature stress (Fig. S2), indicating that the *EPFL6* expression does not depend on a low temperature.

Successful self-pollination at a moderate temperature requires all *EPFL6*-subfamily genes.

In the *Arabidopsis EPFL* family, *EPFL6* and two other genes, *EPFL4* and *EPFL5/CHALLAH-LIKE2*, constitute a subfamily (Abrash et al., 2011; Rychel et al., 2010; Uchida et al., 2012). Previous studies reported that *epfl5/6* double mutant plants failed in the formation of a part of siliques at 22°C, and *epfl4/5/6* triple mutant plants formed almost no siliques (Fig. 4a) (Abrash et al., 2011; Uchida et al., 2012). However, any developmental explanation of the reproduction failure of *epfl4/5/6* has not been given so far. Since we found that *epfl6* plants failed in silique production at a low temperature due to the defect of stamen elongation (Fig. 1), we hypothesized that the reproduction failure of *epfl4/5/6* at a moderate temperature might also be

attributed to the defect of stamen elongation as observed in *epfl6* plants grown at 16°C. To test this hypothesis, we dissected flowers of *epfl4/5/6* grown at 22 °C (Fig. 4b,c). In *epfl4/5/6* flowers, stamens did not grow long enough for anthers to touch the stigma unlike in wild-type plants, and pollens were attached only to the side surface of the pistil distantly apart from the stigma (Fig. 4b,c). We next compared the length and number of filament cells between wild-type and *epfl4/5/6* stamens using flowers with an about 2.5-mm pistil (Fig. 4d). The average length of epidermal cells was similar between wild-type and *epfl4/5/6* (Fig. 4e), while the number of cells that constituted each cell file in *epfl4/5/6* filaments was less than in wild type (Fig. 4f). These results showed that the reduction in the number of filament cells, not cell length, causes the short stamen phenotype of *epfl4/5/6* at 22 °C, as observed in *epfl6* at 16 °C (Fig. 2). Consistent with this phenotype, *EPFL4*, *EPFL5*, and *EPFL6* were all expressed in stamens at 22 °C (Fig. S3). Thus, the entire *EPFL4/5/6* subfamily genes contribute to stamen elongation for successful self-pollination at a moderate temperature.

The receptor protein ERECTA regulates the alignment of the length of stamens and a pistil for self-pollination success.

It was reported that the receptor protein called ERECTA (ER) perceives EPFL4 and EPFL6 peptides in stem development (Uchida et al., 2012). However, it has been unknown whether *ER* plays a role in stamens. When we examined the *ER* expression in reproductive tissues using *ERpro:GUS* reporter plants, *ER* was expressed in stamen filaments as well as pistils (Fig. 5a). The *ER* expression was detected along the line that ran the middle of the filament (Fig. 5a, right panel), suggesting its expression in vascular tissues. This expression pattern was reminiscent of the previous report that *ER* functions in phloem companion cells in inflorescence stems for stem elongation (Uchida et al., 2012; Uchida & Tasaka, 2013). Therefore, we examined whether *ER* is expressed in companion cells of filaments by observing two fluorescent reporters

in filaments, one for the *ER* promoter (Ikematsu et al., 2017) and the other for companion cells (Matsuda et al., 2002). It was reported that the *CoYMV* promoter is active specifically in phloem companion cells of various tissues including filaments (Matsuda et al., 2002; Medberry et al., 1992). The phloem tissue is formed parallel to the xylem tissue developing xylem vessel strands with a characteristic spiral pattern of the secondary cell wall (Fig. 5b, right panel). In filaments, companion cells, which are elongated cells in the phloem tissue, showed *CoYMV* promoter activity (Fig. 5b, nucleus-localized signal). The fluorescence signal derived from the *ER* promoter was specifically detected in the cell with the *CoYMV* promoter activity (Fig. 5b), showing that *ER* is expressed in companion cells of filaments.

If EPFL4/5/6 peptides act on ER to promote stamen elongation like the EPFL4/6-induced stem elongation, *er* mutant plants should show the short stamen phenotype like *epfl6* at 16 °C (Fig. 1) and *epfl4/5/6* at 22 °C (Fig. 4). As expected, stamens developed shorter in *er* flowers than in wild-type flowers at both 22 °C and 16 °C (Figs. 5c, S4a), showing that *ER* promotes stamen elongation. The average lengths of epidermal cells in wild-type and *er* filaments were comparable at the self-pollination stage (Fig. S4b), while the number of cells in each cell file of filaments in *er* was less than in wild type (Fig. S4c). These results demonstrated that the reduction in the number of filament cells in *er*, not cell length, leads to short stamens, phenocopying *epfl6* at 16 °C (Fig. 2) or *epfl4/5/6* at 22 °C (Fig. 4d-f).

Despite the observed short stamens (Fig. 5), no literature has reported that the *er* mutation reduces fertility. This situation was explained by our observation (Fig. 5c,d) that, in *er* flowers at the self-pollination stage, stamens and pistils developed equally short, and anthers were able to deliver pollens to the stigma. These results show that, unlike EPFL4/5/6-subfamily peptides that only promote stamen elongation, ER regulates the elongation of both stamens and pistils. When we examined the *er* mutant plants expressing *ER* by the companion-cell-specific *SUCROSE-PROTON SYMPORTER 2* (*SUC2*) promoter (Imlau et al., 1999), the short stamen

and pistil phenotypes were rescued at both 22 °C and 16 °C (Fig. 5c,d, and S4a), showing that the *ER* activity in companion cells is sufficient for promoting the elongation of both reproductive tissues.

Attenuation of *ER* activity cancels the self-pollination failure due to short stamens.

The *er* mutation led to equally short stamens and pistils, and such flowers accomplished self-pollination since anthers were able to deliver pollens to the stigma (Fig. 5c, S4a). These findings prompted the idea that attenuation of ER activity could cancel the self-pollination failure of mutants with short stamens by additionally shortening pistils and consequently aligning the length of stamens and pistils equally short. To test this idea, we first examined the effect of the *er* mutation on the reproduction failure phenotype of *epfl6* plants grown at 16 °C. In sharp contrast to *epfl6* plants, *epfl6 er* double mutant plants developed siliques (Fig. 6a). In *epfl6 er* flowers, stamen and pistil lengths became almost equal at the self-pollination stage (Fig. 6b), and anthers were able to deliver pollens to the stigma (Fig. 6a). To further examine the ability of the *er* mutation to cancel the self-pollination failure due to short stamens, we next focused on the *myb21* mutant. *MYB21* encodes a transcription factor that promotes filament elongation via a jasmonate-regulated pathway (Song et al., 2011), and *myb21* mutant plants fails in silique production due to reduced elongation of filaments (Fig. 6c,d) (Mandaokar et al., 2006). When we introduced the *er* mutation into the *myb21* mutant, the resulting *myb21 er* double mutant plants developed equally short stamens and pistils and accomplished self-pollination since anthers successfully delivered pollens to the stigma (Fig. 6c,d). These results provided evidence that attenuation of *ER* activity could alleviate the self-pollination insufficiency due to short filaments by aligning the length of stamens and pistils equally short.

Discussion

Conversions between self- and cross-pollination have occurred multiple times within the angiosperms in evolution (Barrett, 2002). The difference between stamen and pistil lengths is one of the developmental traits that underlie such conversions (Kappel et al., 2017; Tedder et al., 2015; Vallejo-Marin & Barrett, 2009). It is also known that environmental changes sometimes induce temporal pollination-type conversions (Kalisz & Vogler, 2003; Kalisz et al., 2004). Furthermore, it has been pointed out that converting the pollination type from cross-pollination to self-pollination could provide an advantage from an agricultural viewpoint because species that can be maintained and propagated by self-pollination are easily stored and distributed as seeds (Cropano et al., 2021; Yang & Mackenzie, 2019). In this study, we showed that the reduction in *EPFL6* activity causes the failure in self-pollination at a cool temperature (Fig. 1). For self-pollinating species, conditional self-pollination failure caused by environmental changes can temporarily prompt occasional cross-pollination, resulting in an increase in genetic diversity (Liu et al., 2019). Although the primary role of *EPFL6* in pollination regulation is considered to confer the robustness of self-pollination success under low-temperature stress, the reduction in the *EPFL6* expression in some environmental conditions may induce occasional cross-pollination to temporally increase the genetic diversity of offspring. The data in this study were collected in well-controlled, stable conditions in plant growth rooms, and we found that the pollen delivery failure of the *epfl6* mutant can be rescued by vigorously shaking flowers by hand (see also the Materials and Methods section). It will be interesting to examine how the *epfl6* phenotype is affected in natural conditions where flowers are randomly shaken by the wind and/or other physical stimulations and monitor whether the self-pollination failure phenotype will enhance cross-pollination tendency in pollinator-existing natural conditions.

Attenuation of ER activity can alleviate the self-pollination insufficiency of mutants with short stamens, such as *myb21*, by additionally shortening pistils and, consequently, aligning the length of stamens and pistils equally short (Fig. 6). This phenomenon prompts the idea that the pollination type of some mutants or plant species with an enhanced cross-pollination tendency because of short stamens can be converted toward the self-pollination type by temporary or constitutive reductions in *ER* activity. It would be intriguing to investigate whether some environmental conditions induce conversions between self- and cross-pollination types through modulation of the *EPFL6*-*ER* pathway and whether evolutionary traces of such conversions can be detected.

The reason why *EPFL6* only promotes stamen elongation, not pistil elongation (Fig. 1), while *ER* mediates the elongation of pistils in addition to stamens (Fig. 5), is likely because of the difference in the expression pattern of these genes. *ER* is strongly expressed in both stamens and pistils (Fig. 5a), while *EPFL6* is preferentially expressed in stamens (Fig. 3a). Because EPFL6 peptides activate ER protein only in stamens, the *epfl6* mutation affects only stamens. On the other hand, it was reported that *EPFL2* and *EPFL9*, which are expressed in pistils, regulate pistil growth via ER (Kawamoto et al., 2020). In the *er* mutant, loss of ER activity in both stamens and pistils leads to insufficient elongation of both tissues.

EPFL6 activates the proliferation of filament cells so that the filament tissue elongates to the appropriate length for self-pollination success at a low temperature (Figs. 1 and 2). Although the *EPFL6* expression does not depend on a low temperature (Fig. S2), filament cells of the *epfl6* mutant show a reduction in proliferation only at a low temperature. Because low-temperature stress generally diminishes cellular activities, including cell proliferation, in various plant tissues (de Jonge et al., 2016; Harrison et al., 1998; Zhu et al., 2015) and temperature stress sometimes causes insufficient development of reproductive tissues (Hedhly et al., 2009; Herrero, 2003), the proliferation activity of filament cells could also be sensitive

391 to low-temperature stress. It would be reasonable to hypothesize that such filament cells with
392 lower cellular activities at a low temperature need to be more provoked to proliferate enough
393 for successful self-pollination than at a moderate temperature. In other words, filament cells
394 may be more sensitive to a reduction in growth-promoting stimuli at a low temperature than at
395 a moderate temperature, which is consistent with the fact that loss of *EPFL6* affects stamen
396 elongation only at a low temperature, not at a moderate temperature (Fig. 1).

397 It was reported that *EPFL4* and *EPFL6* promote elongation of inflorescence stems
398 (Abrash et al., 2011; Uchida et al., 2012). Intriguingly, in either case of stamen or stem, *ER*
399 activity in phloem companion cells promotes tissue growth by activating the proliferation of
400 cells in the tissue. Although a molecular mechanism of how the *ER* activity in companion cells
401 affects the growth of the entire tissue is still unclear, a common mechanism, including a non-
402 cell-autonomous effect derived from companion cells, may act in both cases. It has been
403 reported that phytohormones regulate stamen elongation (Acosta & Przybyl, 2019; Marciniak
404 & Przedniczek, 2019; Song et al., 2013), and mutants with reduced signaling of auxin,
405 gibberellin, or jasmonate exhibit short stamen phenotypes (Cheng et al., 2004; Jewell & Browse,
406 2016; Tashiro et al., 2009). These three hormone pathways constitute a highly intertwined
407 system to control stamen elongation, consisting of transcriptional control, protein interactions,
408 and the transport of hormones (Acosta & Przybyl, 2019; Reeves et al., 2012). It may be
409 noteworthy that gibberellin deficient mutant plants exhibited a reduction in cell number in the
410 stamen filament (Cheng et al., 2004) like *epfl6* and *er* mutants, though the cell length of the
411 filament epidermis was also reduced unlike *epfl6* and *er* mutants. A previous study on the
412 *EPFL4/6*-mediated inflorescence stem growth suggested that gibberellin metabolism might be
413 affected in stems in *epfl4/6* or *er* mutants (Uchida et al., 2012). Combined with the fact that *ER*
414 activity in phloem companion cells commonly promotes the elongation of both filaments and

stems, gibberellin may be a key that connects the ER activity in the phloem with filament elongation.

Besides the coordinated elongation of male and female reproductive tissues highlighted in this study, male-female synchrony in other reproductive processes, such as synchronous development of male and female gametes, is also known to be sensitive to environmental stresses (Hedhly et al., 2009; Herrero, 2003; Liu et al., 2019; Lohani et al., 2020; Zinn et al., 2010). A variety of signaling molecules for intercellular communication must be involved in such male-female synchrony phenomena. In most studied cases of secreted peptides, a specific role in a specific phenomenon has been assigned to each peptide. This study provided evidence that secreted peptides that had been recognized as developmental regulators could also be employed in the machinery that confers robustness against environmental stress. More secreted peptides or signaling molecules with known developmental roles may also play unexpected roles in achieving robust male-female synchrony for reproductive success in fluctuating environments.

Acknowledgments

We thank Michitaka Notaguchi for providing *CoYMVpro:H2B-tdTomato* seeds. This work was supported by MEXT/JSPS KAKENHI (Grant numbers JP17H06476, JP20K21422, JP20H04883, JP20H05409, JP20H05905, JP20H05912, and JP21H02503), the Mitsubishi Foundation, and the Asahi Glass Foundation.

Author Contributions

N.U. conceived the project and designed experiments; S.N., T.H., R.I., and N.U. performed research and analyzed data; S.N., R.I., K.U.T., and N.U. developed and provided materials; N.U. wrote the manuscript; K.U.T., and N.U. edited the manuscript.

Declaration of interests

The authors declare no competing interests.

Supporting Information

Figure S1

Effects of *epfl4* and *epfl6* single mutations on successful self-pollination at 16 °C and 22 °C.

Figure S2

EPFL6 expression levels in filaments at 16 °C and 22 °C.

Figure S3

EPFL4, *EPFL5* and *EPFL6* are expressed in filaments.

Figure S4

Effects of *er* mutation on successful self-pollination at 16 °C and the length and number of filament cells at 22 °C.

Table S1

List of plasmids constructed in this study

Table S2

List of primers used in this study

References

Abrash, E. B., Davies, K. A., & Bergmann, D. C. (2011). Generation of signaling specificity in Arabidopsis by spatially restricted buffering of ligand-receptor interactions. *Plant Cell,* **23**(8), 2864-2879.

Acosta, I. F., & Przybyl, M. (2019). Jasmonate Signaling during Arabidopsis Stamen Maturation. *Plant Cell Physiol,* **60**(12), 2648-2659.

Barrett, S. C. (2002). The evolution of plant sexual diversity. *Nat Rev Genet,* **3**(4), 274-284.

Bessho-Uehara, K., Wang, D. R., Furuta, T., Minami, A., Nagai, K., Gamuyao, R., . . . Ashikari, M. (2016). Loss of function at RAE2, a previously unidentified EPFL, is required for awnlessness in cultivated Asian rice. *Proc Natl Acad Sci U S A,* **113**(32), 8969-8974.

Bowman, J. L. (1994). *Arabidopsis: An Atlas of Morphology and Development*. New York: Springer-Verlag.

Casal, J. J., & Balasubramanian, S. (2019). Thermomorphogenesis. *Annu Rev Plant Biol,* **70**, 321-346.

Cheng, H., Qin, L., Lee, S., Fu, X., Richards, D. E., Cao, D., . . . Peng, J. (2004). Gibberellin regulates Arabidopsis floral development via suppression of DELLA protein function. *Development,* **131**(5), 1055-1064.

Clough, S. J., & Bent, A. F. (1998). Floral dip: a simplified method for Agrobacterium-mediated transformation of Arabidopsis thaliana. *Plant J,* **16**(6), 735-743.

Cropano, C., Place, I., Manzanares, C., Do Canto, J., Lubberstedt, T., Studer, B., & Thorogood, D. (2021). Characterization and practical use of self-compatibility in outcrossing grass species. *Ann Bot,* **127**(7), 841-852.

de Jonge, J., Kodde, J., Severing, E. I., Bonnema, G., Angenent, G. C., Immink, R. G., & Groot, S. P. (2016). Low Temperature Affects Stem Cell Maintenance in Brassica oleracea Seedlings. *Front Plant Sci,* **7**, 800.

Ding, Y., Shi, Y., & Yang, S. (2020). Molecular Regulation of Plant Responses to Environmental Temperatures. *Mol Plant,* **13**(4), 544-564.

Fattorini, R., & Glover, B. J. (2020). Molecular Mechanisms of Pollination Biology. *Annu Rev Plant Biol,* **71**, 487-515.

Gray, S. B., & Brady, S. M. (2016). Plant developmental responses to climate change. *Dev Biol,* **419**(1), 64-77.

Haider, S., Iqbal, J., Naseer, S., Yaseen, T., Shaukat, M., Bibi, H., . . . Mahmood, T. (2021). Molecular mechanisms of plant tolerance to heat stress: current landscape and future perspectives. *Plant Cell Rep,* **40**(12), 2247-2271.

Hara, K., Kajita, R., Torii, K. U., Bergmann, D. C., & Kakimoto, T. (2007). The secretory peptide gene EPF1 enforces the stomatal one-cell-spacing rule. *Genes Dev,* **21**(14), 1720-1725.

Hara, K., Yokoo, T., Kajita, R., Onishi, T., Yahata, S., Peterson, K. M., . . . Kakimoto, T. (2009). Epidermal cell density is autoregulated via a secretory peptide, EPIDERMAL PATTERNING FACTOR 2 in Arabidopsis leaves. *Plant Cell Physiol,* **50**(6), 1019-1031.

Harrison, J., Nicot, C., & Ougham, H. (1998). The effect of low temperature on patterns of cell division in developing second leaves of wild-type and slender mutant barley (Hordeum vulgare L.). *Plant Cell and Environment,* **21**(1), 79-86.

Hedhly, A., Hormaza, J. I., & Herrero, M. (2009). Global warming and sexual plant reproduction. *Trends Plant Sci,* **14**(1), 30-36.

Herrero, M. (2003). Male and female synchrony and the regulation of mating in flowering plants. *Philos Trans R Soc Lond B Biol Sci,* **358**(1434), 1019-1024.

Hunt, L., Bailey, K. J., & Gray, J. E. (2010). The signalling peptide EPFL9 is a positive regulator of stomatal development. *New Phytol,* **186**(3), 609-614.

Hunt, L., & Gray, J. E. (2009). The signaling peptide EPF2 controls asymmetric cell divisions during stomatal development. *Curr Biol,* **19**(10), 864-869.

Ikematsu, S., Tasaka, M., Torii, K. U., & Uchida, N. (2017). ERECTA-family receptor kinase genes redundantly prevent premature progression of secondary growth in the Arabidopsis hypocotyl. *New Phytol,* **213**(4), 1697-1709.

Imlau, A., Truernit, E., & Sauer, N. (1999). Cell-to-cell and long-distance trafficking of the green fluorescent protein in the phloem and symplastic unloading of the protein into sink tissues. *Plant Cell,* **11**(3), 309-322.

Jewell, J. B., & Browse, J. (2016). Epidermal jasmonate perception is sufficient for all aspects of jasmonate-mediated male fertility in Arabidopsis. *Plant J,* **85**(5), 634-647.

Kalisz, S., & Vogler, D. W. (2003). Benefits of autonomous selfing under unpredictable pollinator environments. *Ecology,* **84**(11), 2928-2942.

Kalisz, S., Vogler, D. W., & Hanley, K. M. (2004). Context-dependent autonomous self-fertilization yields reproductive assurance and mixed mating. *Nature,* **430**(7002), 884-887.

Kappel, C., Huu, C. N., & Lenhard, M. (2017). A short story gets longer: recent insights into the molecular basis of heterostyly. *J Exp Bot,* **68**(21-22), 5719-5730.

Kawamoto, N., Del Carpio, D. P., Hofmann, A., Mizuta, Y., Kurihara, D., Higashiyama, T., . . . Simon, R. (2020). A Peptide Pair Coordinates Regular Ovule Initiation Patterns with Seed Number and Fruit Size. *Curr Biol,* **30**(22), 4352-4361 e4354.

Kondo, T., Kajita, R., Miyazaki, A., Hokoyama, M., Nakamura-Miura, T., Mizuno, S., . . . Sakagami, Y. (2010). Stomatal density is controlled by a mesophyll-derived signaling molecule. *Plant Cell Physiol,* **51**(1), 1-8.

Kosentka, P. Z., Overholt, A., Maradiaga, R., Mitoubsi, O., & Shpak, E. D. (2019). EPFL Signals in the Boundary Region of the SAM Restrict Its Size and Promote Leaf Initiation. *Plant Physiol,* **179**(1), 265-279.

Kumar, V., Belavadi, V. V., Revanasidda, Tharini, K. B., & Srinivasa, Y. B. (2019). Stamen elongation in sunn hemp appears to allow delayed self-pollination in the absence of pollinators - A case of bet-hedging? *South African Journal of Botany,* **127**, 110-116.

573 Kurihara, D., Mizuta, Y., Sato, Y., & Higashiyama, T. (2015). ClearSee: a rapid optical clearing
574 reagent for whole-plant fluorescence imaging. *Development,* **142**(23), 4168-4179.
575
576 Lamers, J., van der Meer, T., & Testerink, C. (2020). How Plants Sense and Respond to
577 Stressful Environments. *Plant Physiol,* **182**(4), 1624-1635.
578
579 Lee, J. S., Hnilova, M., Maes, M., Lin, Y. C., Putarjunan, A., Han, S. K., . . . Torii, K. U. (2015).
580 Competitive binding of antagonistic peptides fine-tunes stomatal patterning. *Nature,*
581 **522**(7557), 439-443.
582
583 Lee, J. S., Kuroha, T., Hnilova, M., Khatayevich, D., Kanaoka, M. M., McAbee, J. M., . . . Torii,
584 K. U. (2012). Direct interaction of ligand-receptor pairs specifying stomatal patterning.
585 *Genes Dev,* **26**(2), 126-136.
586
587 Liu, B., Mo, W. J., Zhang, D., De Storme, N., & Geelen, D. (2019). Cold Influences Male
588 Reproductive Development in Plants: A Hazard to Fertility, but a Window for Evolution.
589 *Plant Cell Physiol,* **60**(1), 7-18.
590
591 Lohani, N., Singh, M. B., & Bhalla, P. L. (2020). High temperature susceptibility of sexual
592 reproduction in crop plants. *J Exp Bot,* **71**(2), 555-568.
593
594 Mandaokar, A., Thines, B., Shin, B., Lange, B. M., Choi, G., Koo, Y. J., . . . Browse, J. (2006).
595 Transcriptional regulators of stamen development in Arabidopsis identified by
596 transcriptional profiling. *Plant J,* **46**(6), 984-1008.
597
598 Marciniak, K., & Przedniczek, K. (2019). Comprehensive Insight into Gibberellin- and
599 Jasmonate-Mediated Stamen Development. *Genes (Basel),* **10**(10).
600
601 Matsuda, Y., Liang, G., Zhu, Y., Ma, F., Nelson, R. S., & Ding, B. (2002). The Commelina
602 yellow mottle virus promoter drives companion-cell-specific gene expression in
603 multiple organs of transgenic tobacco. *Protoplasma,* **220**(1-2), 51-58.
604
605 Medberry, S. L., Lockhart, B. E., & Olszewski, N. E. (1992). The Commelina yellow mottle
606 virus promoter is a strong promoter in vascular and reproductive tissues. *Plant Cell,*
607 **4**(2), 185-192.
608

609 Reeves, P. H., Ellis, C. M., Ploense, S. E., Wu, M. F., Yadav, V., Tholl, D., . . . Reed, J. W.
610 (2012). A regulatory network for coordinated flower maturation. *PLoS Genet,* **8**(2),
611 e1002506.
612
613 Rychel, A. L., Peterson, K. M., & Torii, K. U. (2010). Plant twitter: ligands under 140 amino
614 acids enforcing stomatal patterning. *J Plant Res,* **123**(3), 275-280.
615
616 Schneider, C. A., Rasband, W. S., & Eliceiri, K. W. (2012). NIH Image to ImageJ: 25 years of
617 image analysis. *Nat Methods,* **9**(7), 671-675.
618
619 Shpak, E. D., Berthiaume, C. T., Hill, E. J., & Torii, K. U. (2004). Synergistic interaction of
620 three ERECTA-family receptor-like kinases controls Arabidopsis organ growth and
621 flower development by promoting cell proliferation. *Development,* **131**(7), 1491-1501.
622
623 Song, S., Qi, T., Huang, H., Ren, Q., Wu, D., Chang, C., . . . Xie, D. (2011). The Jasmonate-
624 ZIM domain proteins interact with the R2R3-MYB transcription factors MYB21 and
625 MYB24 to affect Jasmonate-regulated stamen development in Arabidopsis. *Plant Cell,*
626 **23**(3), 1000-1013.
627
628 Song, S., Qi, T., Huang, H., & Xie, D. (2013). Regulation of stamen development by
629 coordinated actions of jasmonate, auxin, and gibberellin in Arabidopsis. *Mol Plant,* **6**(4),
630 1065-1073.
631
632 Sugano, S. S., Shimada, T., Imai, Y., Okawa, K., Tamai, A., Mori, M., & Hara-Nishimura, I.
633 (2010). Stomagen positively regulates stomatal density in Arabidopsis. *Nature,*
634 **463**(7278), 241-244.
635
636 Takata, N., Yokota, K., Ohki, S., Mori, M., Taniguchi, T., & Kurita, M. (2013). Evolutionary
637 relationship and structural characterization of the EPF/EPFL gene family. *PLoS One,*
638 **8**(6), e65183.
639
640 Tameshige, T., Ikematsu, S., Torii, K. U., & Uchida, N. (2017). Stem development through
641 vascular tissues: EPFL-ERECTA family signaling that bounces in and out of phloem. *J*
642 *Exp Bot,* **68**(1), 45-53.
643
644 Tameshige, T., Okamoto, S., Lee, J. S., Aida, M., Tasaka, M., Torii, K. U., & Uchida, N. (2016).
645 A Secreted Peptide and Its Receptors Shape the Auxin Response Pattern and Leaf
646 Margin Morphogenesis. *Curr Biol,* **26**(18), 2478-2485.

Tashiro, S., Tian, C. E., Watahiki, M. K., & Yamamoto, K. T. (2009). Changes in growth kinetics of stamen filaments cause inefficient pollination in massugu2, an auxin insensitive, dominant mutant of Arabidopsis thaliana. *Physiol Plant,* **137**(2), 175-187.

Tedder, A., Carleial, S., Golebiewska, M., Kappel, C., Shimizu, K. K., & Stift, M. (2015). Evolution of the Selfing Syndrome in Arabis alpina (Brassicaceae). *PLoS One,* **10**(6), e0126618.

Torii, K. U., Mitsukawa, N., Oosumi, T., Matsuura, Y., Yokoyama, R., Whittier, R. F., & Komeda, Y. (1996). The Arabidopsis ERECTA gene encodes a putative receptor protein kinase with extracellular leucine-rich repeats. *Plant Cell,* **8**(4), 735-746.

Uchida, N., Igari, K., Bogenschutz, N. L., Torii, K. U., & Tasaka, M. (2011). Arabidopsis ERECTA-family receptor kinases mediate morphological alterations stimulated by activation of NB-LRR-type UNI proteins. *Plant Cell Physiol,* **52**(5), 804-814.

Uchida, N., Lee, J. S., Horst, R. J., Lai, H. H., Kajita, R., Kakimoto, T., . . . Torii, K. U. (2012). Regulation of inflorescence architecture by intertissue layer ligand-receptor communication between endodermis and phloem. *Proc Natl Acad Sci U S A,* **109**(16), 6337-6342.

Uchida, N., & Tasaka, M. (2013). Regulation of plant vascular stem cells by endodermis-derived EPFL-family peptide hormones and phloem-expressed ERECTA-family receptor kinases. *J Exp Bot,* **64**(17), 5335-5343.

Vallejo-Marin, M., & Barrett, S. C. (2009). Modification of flower architecture during early stages in the evolution of self-fertilization. *Ann Bot,* **103**(6), 951-962.

Yang, X., & Mackenzie, S. A. (2019). Many Facets of Dynamic Plasticity in Plants. *Cold Spring Harb Perspect Biol,* **11**(10).

Zhu, J., Zhang, K. X., Wang, W. S., Gong, W., Liu, W. C., Chen, H. G., . . . Lu, Y. T. (2015). Low Temperature Inhibits Root Growth by Reducing Auxin Accumulation via ARR1/12. *Plant and Cell Physiology,* **56**(4), 727-736.

Zinn, K. E., Tunc-Ozdemir, M., & Harper, J. F. (2010). Temperature stress and plant sexual reproduction: uncovering the weakest links. *J Exp Bot,* **61**(7), 1959-1968.

Figure legends

Figure 1. *EPFL6* ensures self-pollination success at a cool temperature by promoting stamen growth.

(a) Inflorescences of plants grown at indicated temperatures. Asterisks show the failure of the formation of siliques. Scale bar, 1 cm. **(b)** Flowers with an about 2.5-mm pistil are shown as samples at the developmental stage suitable for self-pollination. Plants were grown at 16 °C. Sepals and petals were removed to observe stamens and a pistil of each flower. Lower panels show enlarged images near the stamen tip. The double-headed arrows indicate successful pollination between stamens and the pistil of the nearly same length. Arrows indicate pollen attachment to the stigma or the pistil's side surface distantly apart from the stigma. Scale bar, 0.5 mm. **(c, d)** Scatter plots showing the relation between stamen and pistil lengths in flowers of WT and *epfl6* plants grown at 22 °C or 16 °C. Each dot indicates the lengths of the pistil and the longest stamen in a single flower. If the stamen length is nearly equal to the pistil length, such dot is located on or close to the diagonal line, showing a high expectation of successful pollination. Flowers at various developmental stages were collected from plants grown in multiple batches.

Figure 2. *EPFL6* promotes cell proliferation of stamen filaments at a cool temperature.

(a) Cleared filaments from flowers with an about 2.5-mm pistil. WT and *epfl6* were grown at 16 °C. Dots indicate cells constituting a representative cell file in the filament epidermis. Scale bar, 0.2 mm. Representative cells are colored gray with dotted outlines in enlarged images. Scale bar, 0.1 mm. **(b)** Length of cells in the filament epidermis from flowers with an about 2.5-mm pistil. Cell length along the long axis of the filament was measured using eight filaments from four flowers (two long stamens were randomly chosen per flower). Dots indicate

the length of each cell. Box-and-whisker plots show a median (centerline), upper/lower quartiles (box limits), and maximum/minimum (upper/lower whiskers). Black dots indicate outliers. Outlines of violin plots are also drawn. P-values were determined by a Welch's t-test (two-tailed). **(c)** Number of cells per cell file of the filament epidermis from flowers with an about 2.5-mm pistil. WT and *epfl6* were grown at 16 °C. Cells from the bottom end to the top end of each cell file were counted using sixteen files from four flowers (four long stamens per flower). Dots indicate the number of cells included in each file. Box-and-whisker plots show a median (centerline), upper/lower quartiles (box limits), and maximum/minimum (upper/lower whiskers). Outlines of violin plots are also drawn. P-values were determined by a Welch's t-test (two-tailed).

Figure 3. *EPFL6* expression in filaments is sufficient for self-pollination success at a cool temperature.

(a, c, e) GUS-stained inflorescences and flowers from plants grown at 16 °C. Samples were cleared by chloral hydrate. Sepals and petals were removed from the cleared flowers to observe stamens and a pistil of each flower. Black arrowheads indicate GUS signals in inflorescence stems. Red arrowheads indicate GUS signals in stamen filaments. Scale bar, 2 mm for inflorescence images and 0.5 mm for flower images. **(b, d, f)** Inflorescences of plants grown at 16 °C. Asterisks show the failure of the formation of siliques. Scale bar, 1 cm.

Figure 4. Successful self-pollination at a moderate temperature requires all *EPFL6*-subfamily genes.

(a) Inflorescences of plants grown at 22 °C. Asterisks show the failure of the formation of siliques. Scale bar, 1 cm. **(b)** Flowers with an about 2.5-mm pistil are shown as samples at the developmental stage suitable for self-pollination. Sepals and petals were removed to observe

735 stamens and a pistil of each flower. Lower panels show enlarged images near the stamen tip.
736 The double-headed arrow in the WT panel indicates successful pollination between stamens
737 and the pistil of the nearly same length. Stamens do not elongate enough to reach the stigma at
738 the tip of the pistil in *epfl4/5/6*. Arrows indicate pollen attachment to the stigma in WT and the
739 pistil's side surface distantly apart from the stigma in *epfl4/5/6*. Scale bar, 0.5 mm. **(c)** Scatter
740 plots showing the relation between stamen and pistil lengths. Each dot indicates the lengths of
741 the pistil and the longest stamen in a single flower. If the stamen length is nearly equal to the
742 pistil length, such dot is located on or close to the diagonal line, showing a high expectation of
743 successful pollination. Flowers at various developmental stages were collected from plants
744 grown in multiple batches. **(d)** Cleared filaments from flowers with an about 2.5-mm pistil.
745 Representative cells are colored gray with dotted outlines. Scale bar, 0.2 mm. **(e)** Length of
746 cells in the filament epidermis from flowers with an about 2.5-mm pistil. Cell length along the
747 long axis of the filament was measured using eight filaments from four flowers (two long
748 stamens were randomly chosen per flower). Dots indicate the length of each cell. Box-and-
749 whisker plots show a median (centerline), upper/lower quartiles (box limits), and
750 maximum/minimum (upper/lower whiskers). Black dots indicate outliers. Outlines of violin
751 plots are also drawn. P-values were determined by a Welch's t-test (two-tailed). **(f)** Number of
752 cells per cell file of the filament epidermis from flowers with an about 2.5-mm pistil. Cells from
753 the bottom end to the top end of each cell file were counted using sixteen files from four flowers
754 (four long stamens per flower). Dots indicate the number of cells included in each file. Box-
755 and-whisker plots show a median (centerline), upper/lower quartiles (box limits), and
756 maximum/minimum (upper/lower whiskers). Outlines of violin plots are also drawn. P-values
757 were determined by a Welch's t-test (two-tailed).
758

Figure 5. The receptor kinase ER in phloem cells promotes elongation of stamens and pistils.

(a) A GUS-stained flower from *ERpro:GUS* plants grown at 22 °C. Sepals and petals were removed to observe stamens and a pistil. The black arrowhead indicates GUS signals in the pistil. Red arrowheads indicate GUS signals in stamen filaments. Scale bar, 0.5 mm. **(b)** Fluorescent signals derived from *ERpro:ER-YFP* and *CoYMVpro:H2B-tdTomato* in a filament tissue. A representative photo among more samples than twenty is shown. YFP and tdTomato signals are indicated in blue and magenta, respectively. The original intracellular localization of ER-YFP proteins, which was expected to be detected at the plasma membrane (Ikematsu et al., 2017), was likely disrupted by fixation procedures using a detergent for deep imaging of the filament tissue. The right panel shows fluorescence signals merged with the differential interference contrast (DIC) image. The asterisk indicates a xylem cell file that harbors a spiral pattern of the secondary cell wall. Scale bar, 10 μm. **(c)** Flowers at the developmental stage suitable for self-pollination are shown. Sepals and petals were removed to observe stamens and a pistil of each flower. Double-headed arrows indicate successful pollination between stamens and the pistil of the nearly same length. Scale bar, 0.5 mm. **(d)** Scatter plots showing the relation between stamen and pistil lengths. Each dot in scatter plots indicates the lengths of the pistil and the longest stamen in a single flower. If the stamen length is nearly equal to the pistil length, such dot is located on or close to the diagonal line, showing a high expectation of successful pollination. Flowers at various developmental stages were collected from plants grown in multiple batches.

Figure 6. Attenuation of *ER* activity cancels the self-pollination failure due to short stamens.

(a–d) Flowers at the developmental stage suitable for self-pollination (a, c), and scatter plots showing the relation between stamen and pistil lengths (b, d). Sepals and petals were removed to observe stamens and a pistil of each flower. Each dot in scatter plots indicates the lengths of the pistil and the longest stamen in a single flower. If the stamen length is nearly equal to the pistil length, such dot is located on or close to the diagonal line, showing a high expectation of successful pollination. Flowers at various developmental stages were collected from plants grown in multiple batches. In flower images, double-headed arrows indicate successful pollination between stamens and the pistil of the nearly same length. Arrows indicate pollen attachment to the pistil's side surface distantly apart from the stigma. In inflorescence images, asterisks show the failure of the formation of siliques. Scale bar, 1 cm for inflorescence images and 0.5 mm for flower images.

Figure 1

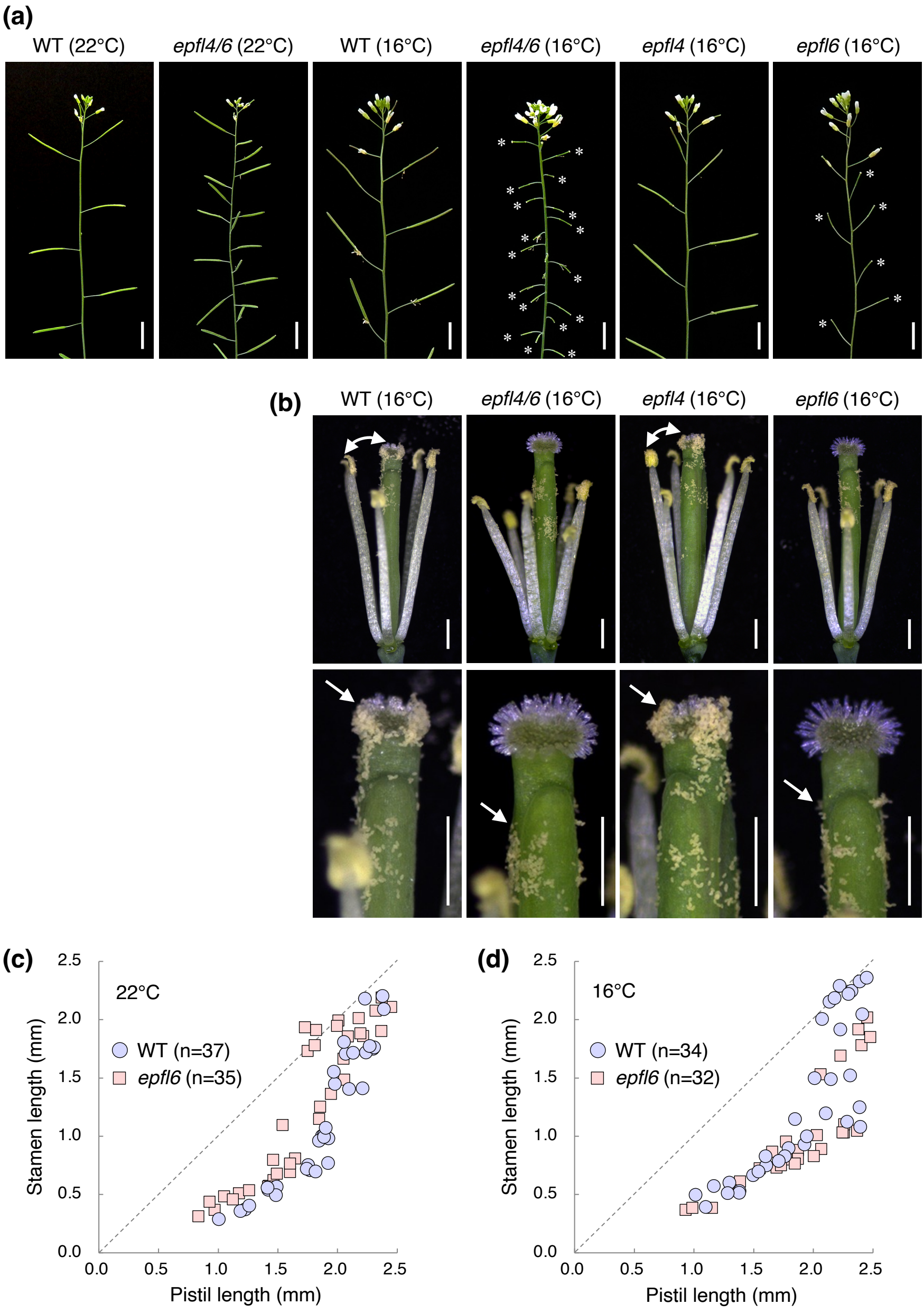
(a)
WT (22°C)
epfl4/6 (22°C)
WT (16°C)
epfl4/6 (16°C)
epfl4 (16°C)
epfl6 (16°C)
(b)
WT (16°C)
epfl4/6 (16°C)
epfl4 (16°C)
epfl6 (16°C)
(c)
22°C
WT (n=37)
epfl6 (n=35)
Stamen length (mm)
Pistil length (mm)
0.0
0.5
1.0
1.5
2.0
2.5
(d)
16°C
WT (n=34)
epfl6 (n=32)
Stamen length (mm)
Pistil length (mm)

Figure 2

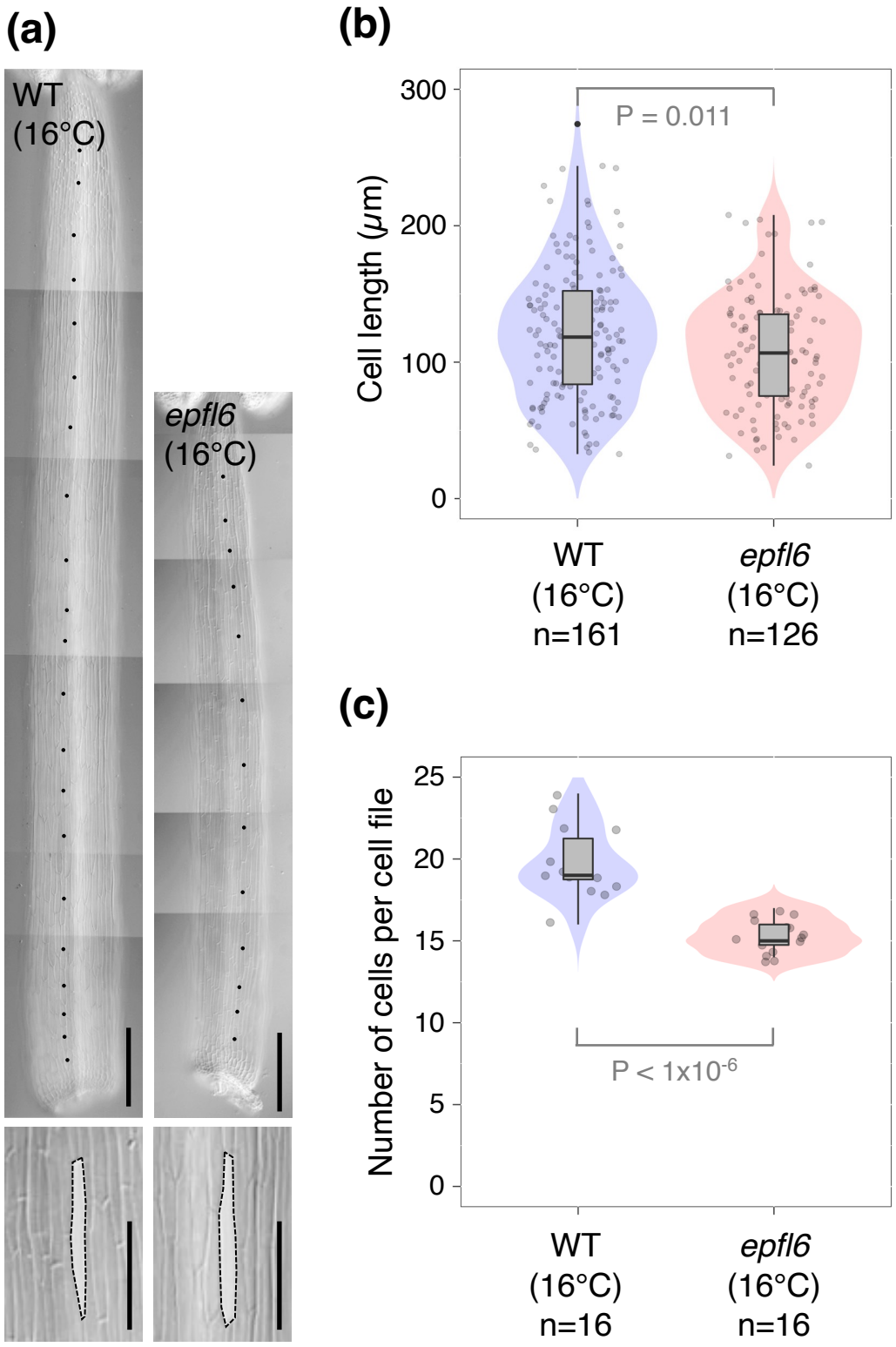
(a)
WT
(16°C)
epfl6
(16°C)
(b)
P = 0.011
Cell length (μm)
300
200
100
0
WT
(16°C)
n=161
epfl6
(16°C)
n=126
(c)
Number of cells per cell file
25
20
15
10
5
0
P < 1x10-6
WT
(16°C)
n=16
epfl6
(16°C)
n=16

Figure 3

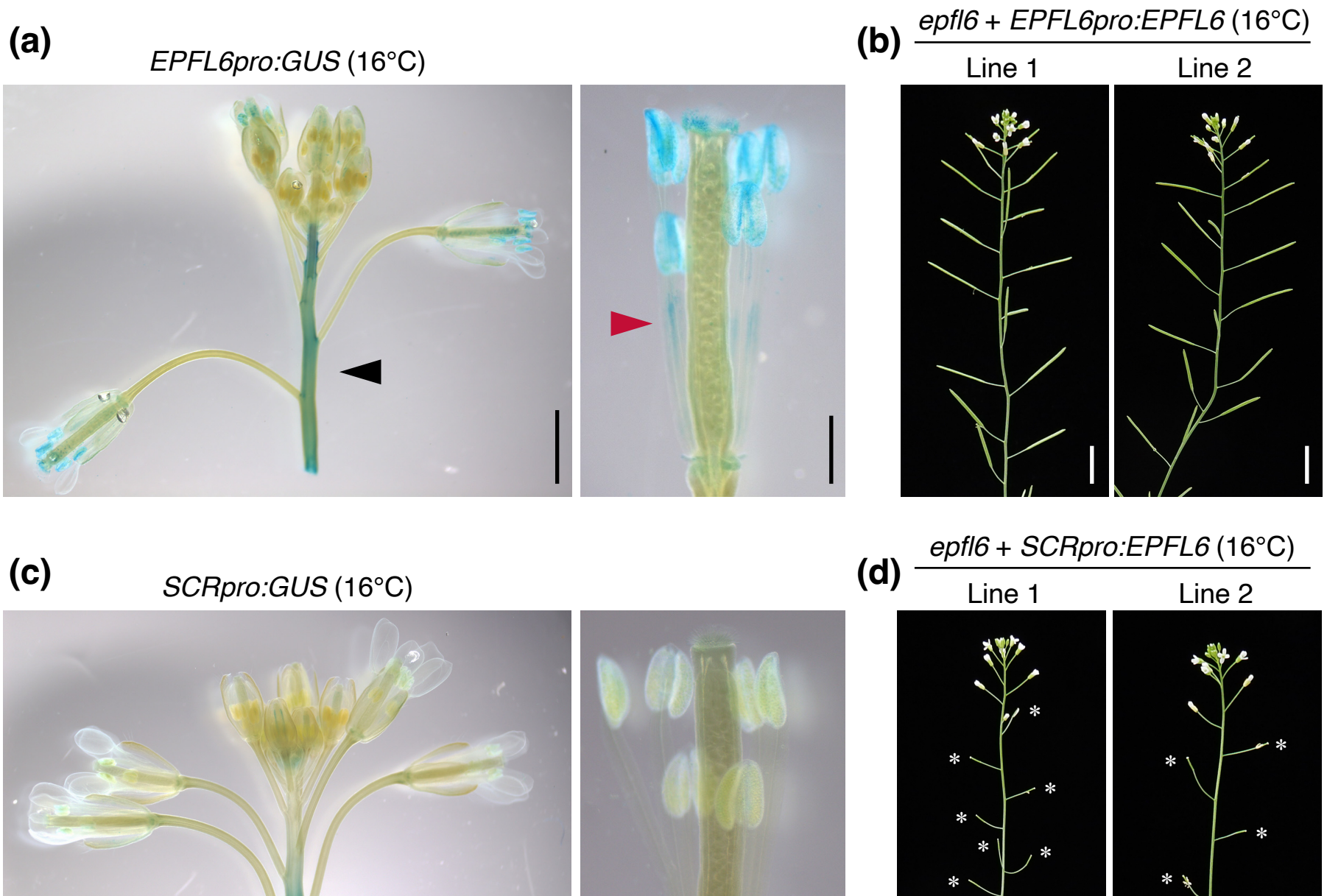
(a)
EPFL6pro:GUS (16°C)
(b)
epfl6 + EPFL6pro:EPFL6 (16°C)
Line 1
Line 2
(c)
SCRpro:GUS (16°C)
(d)
epfl6 + SCRpro:EPFL6 (16°C)
Line 1
Line 2
(e)
IAA19pro:GUS (16°C)
(f)
epfl6 + IAA19pro:EPFL6 (16°C)
Line 1
Line 2

Figure 4

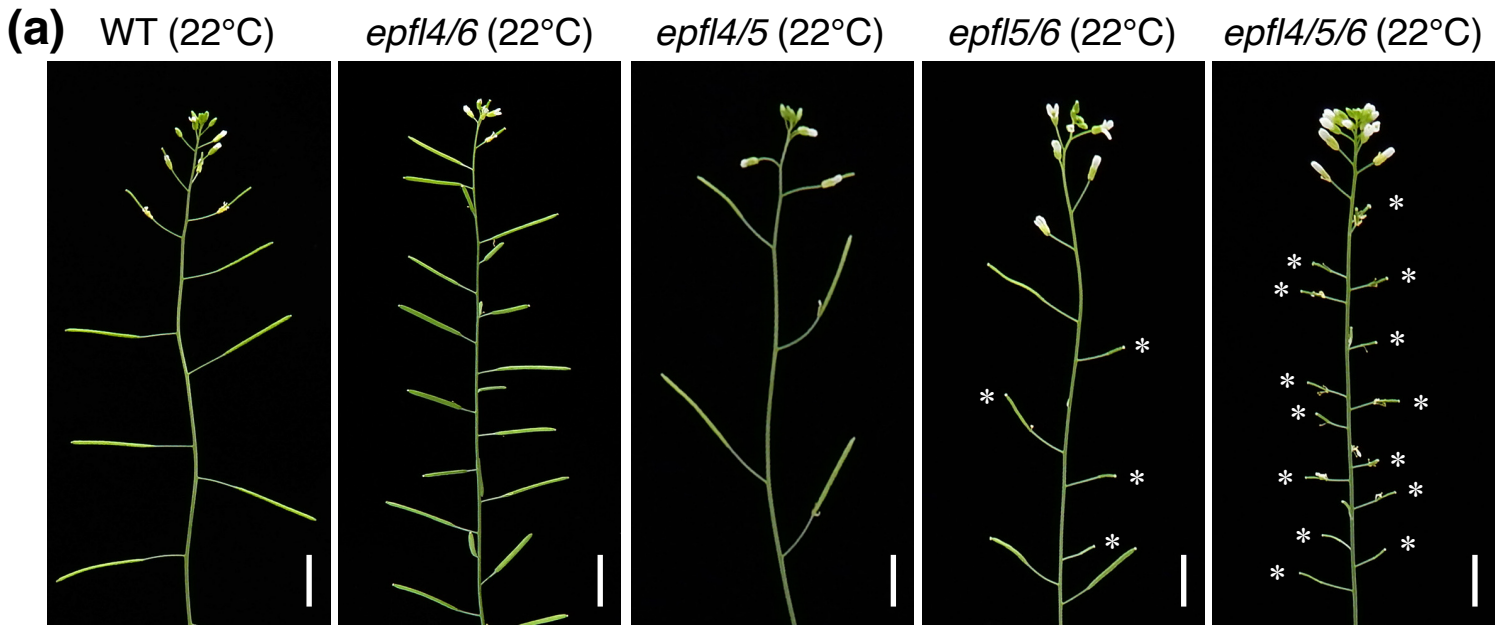
(a)
WT (22°C)
epfl4/6 (22°C)
epfl4/5 (22°C)
epfl5/6 (22°C)
epfl4/5/6 (22°C)

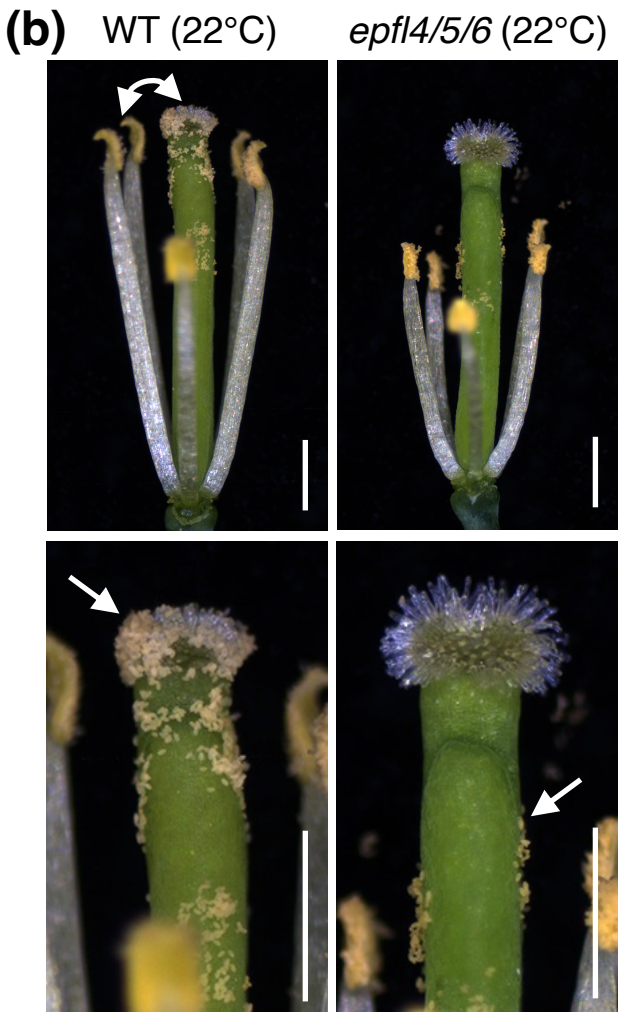
(b)
WT (22°C)
epfl4/5/6 (22°C)

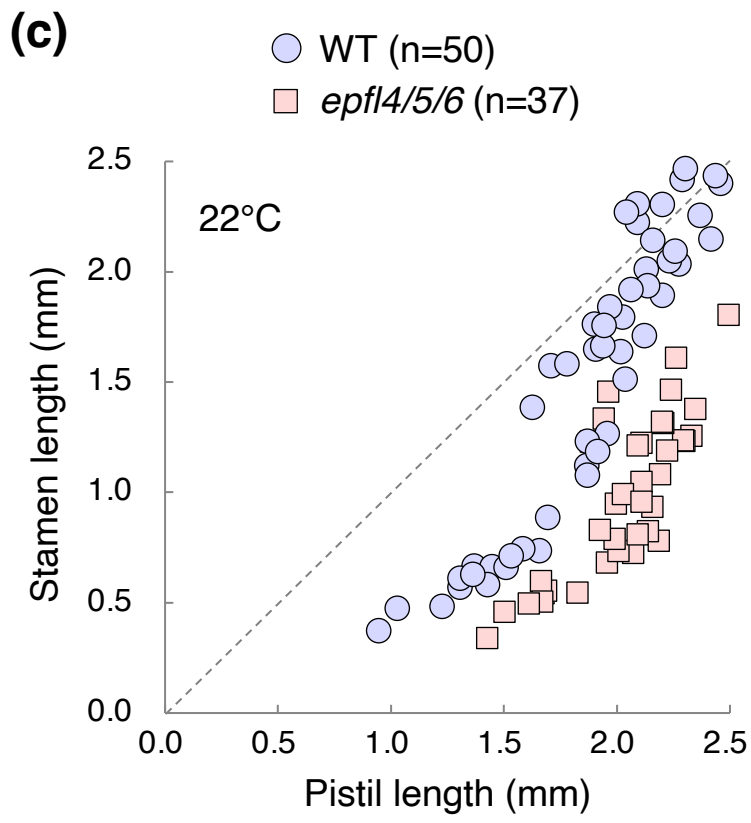
(c)
WT (n=50)
epfl4/5/6 (n=37)
22°C
Stamen length (mm)
Pistil length (mm)
0.0
0.5
1.0
1.5
2.0
2.5

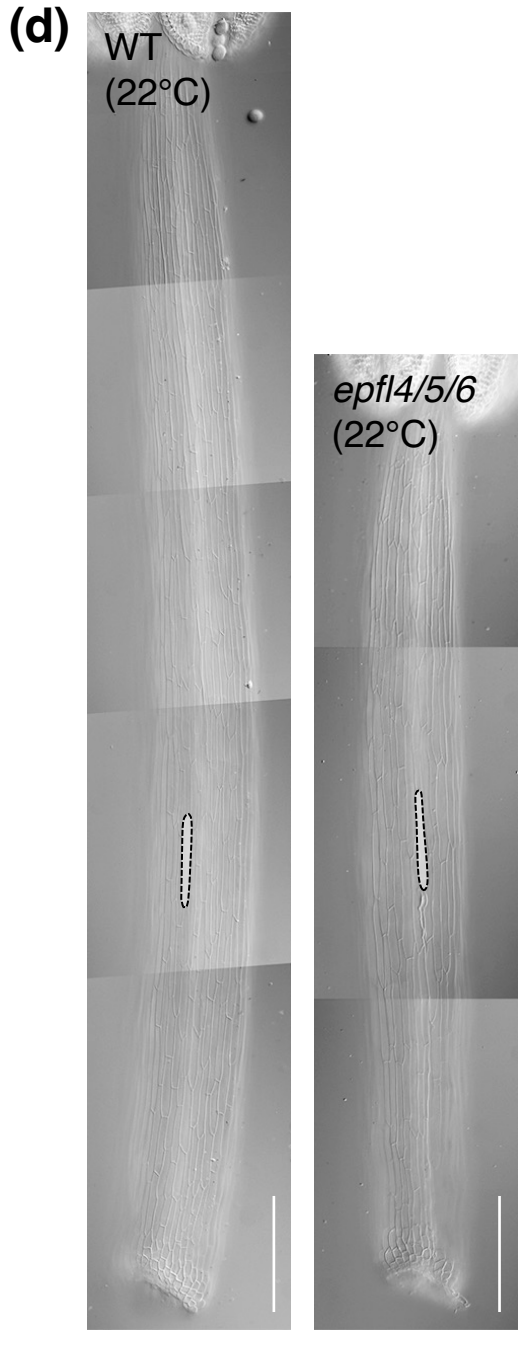
(d)
WT
(22°C)
epfl4/5/6
(22°C)

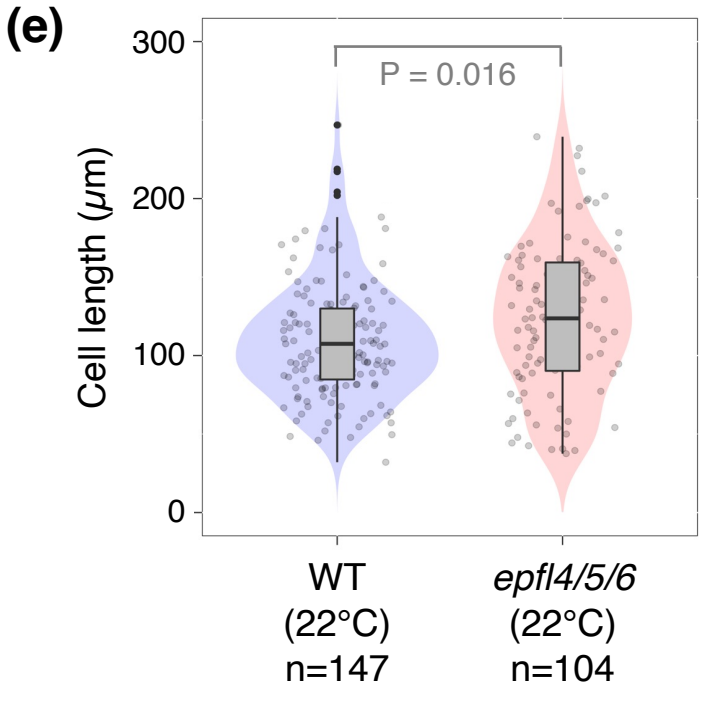
(e)
P = 0.016
Cell length (μm)
0
100
200
300
WT
(22°C)
n=147
epfl4/5/6
(22°C)
n=104

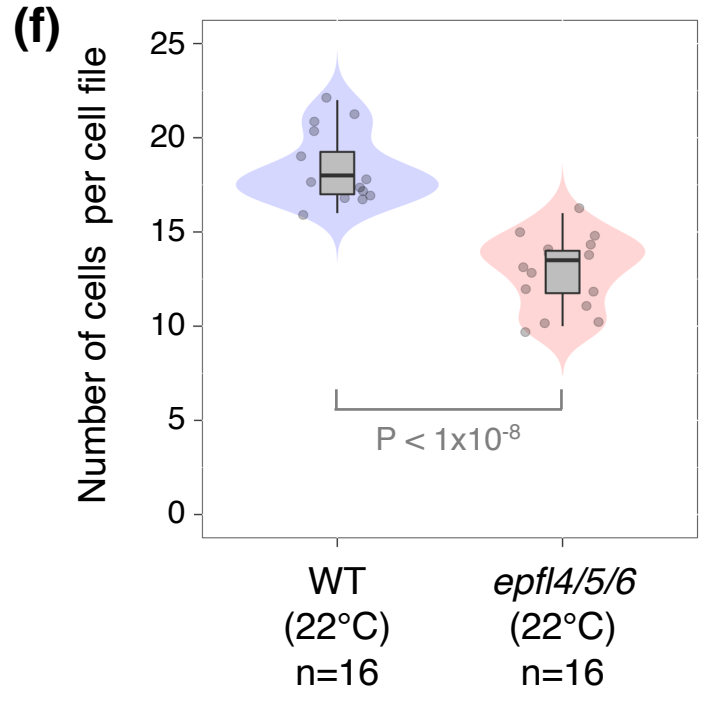
(f)
Number of cells per cell file
0
5
10
15
20
25
P < 1x10-8
WT
(22°C)
n=16
epfl4/5/6
(22°C)
n=16

Figure 5

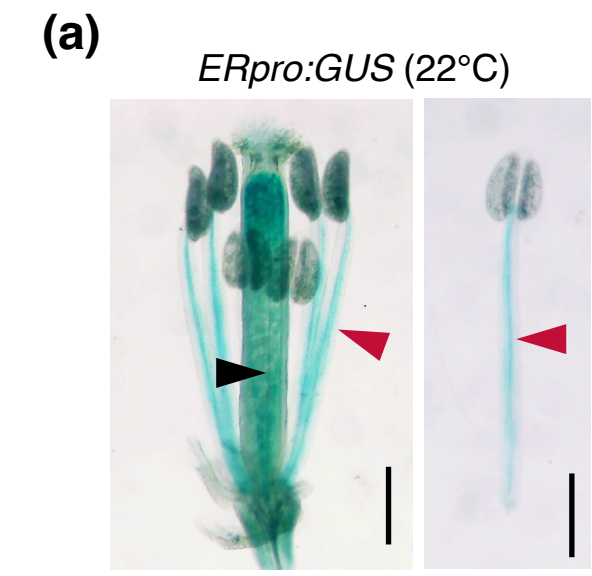
(a)
ERpro:GUS (22°C)

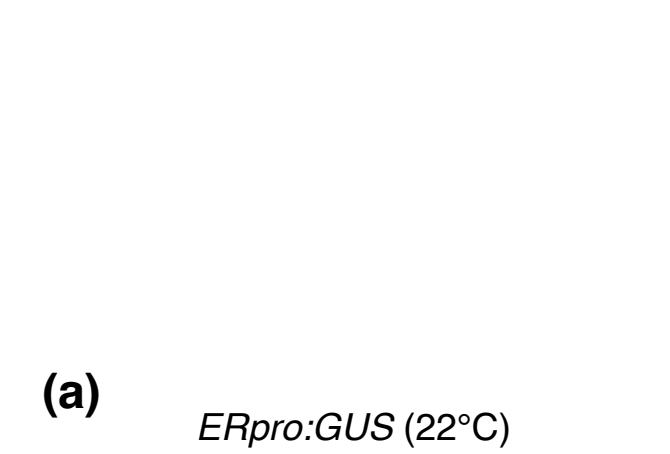
(b)
ERpro:ER-YFP
CoYMVpro:H2B-tdTomato
DIC
*

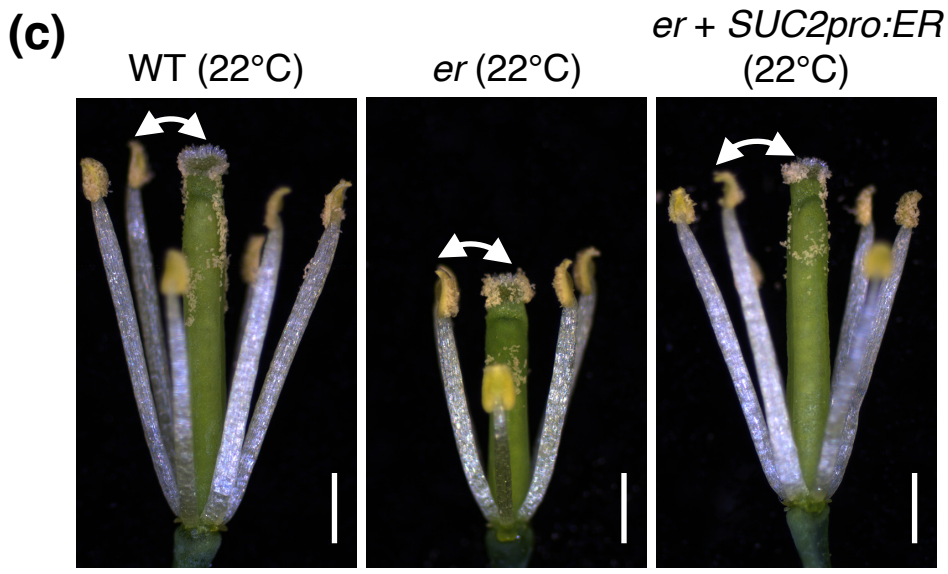
(c)
WT (22°C)
er (22°C)
er + SUC2pro:ER
(22°C)

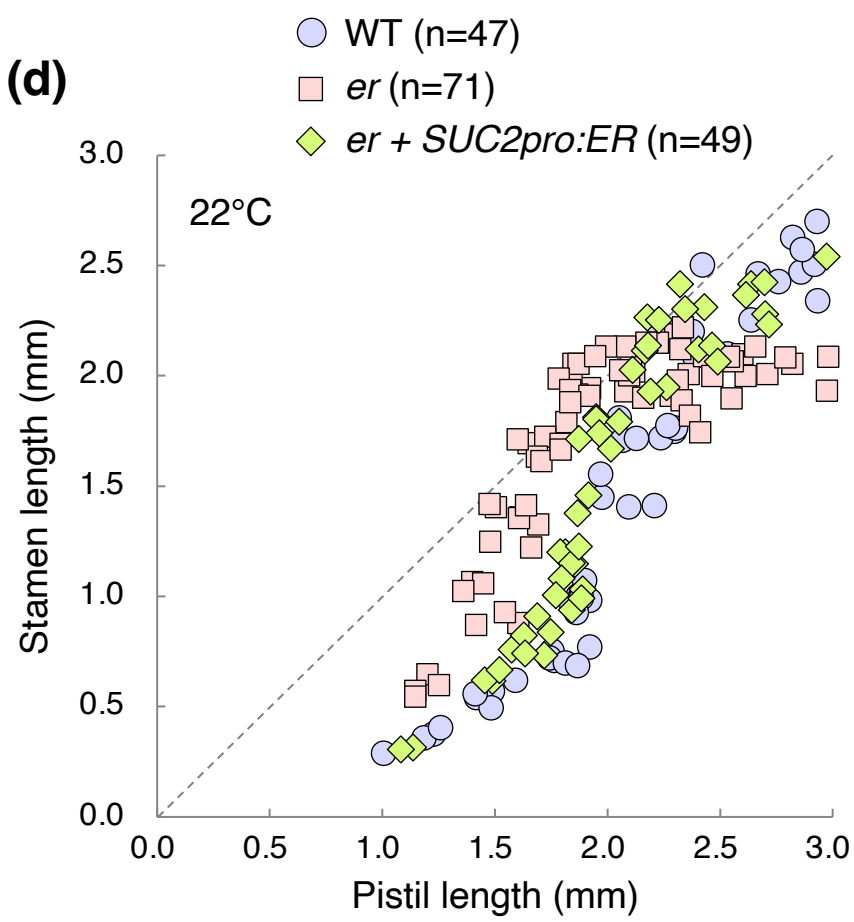
(d)
WT (n=47)
er (n=71)
er + SUC2pro:ER (n=49)
22°C
Stamen length (mm)
Pistil length (mm)
0.0
0.5
1.0
1.5
2.0
2.5
3.0

Figure 6

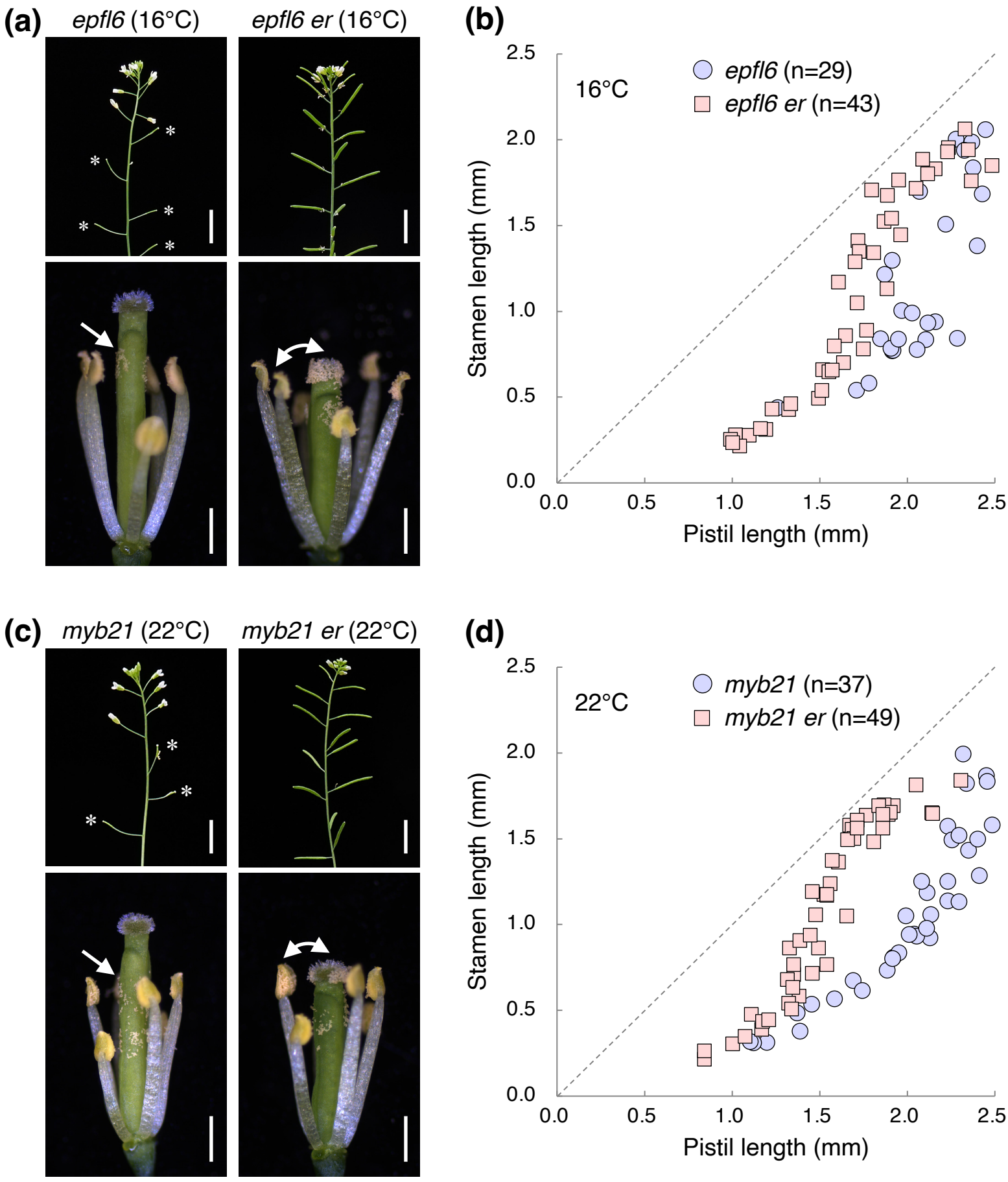
(a)
epfl6 (16°C)
epfl6 er (16°C)
(b)
16°C
epfl6 (n=29)
epfl6 er (n=43)
Stamen length (mm)
Pistil length (mm)
0.0
0.5
1.0
1.5
2.0
2.5
(c)
myb21 (22°C)
myb21 er (22°C)
(d)
22°C
myb21 (n=37)
myb21 er (n=49)
Stamen length (mm)
Pistil length (mm)

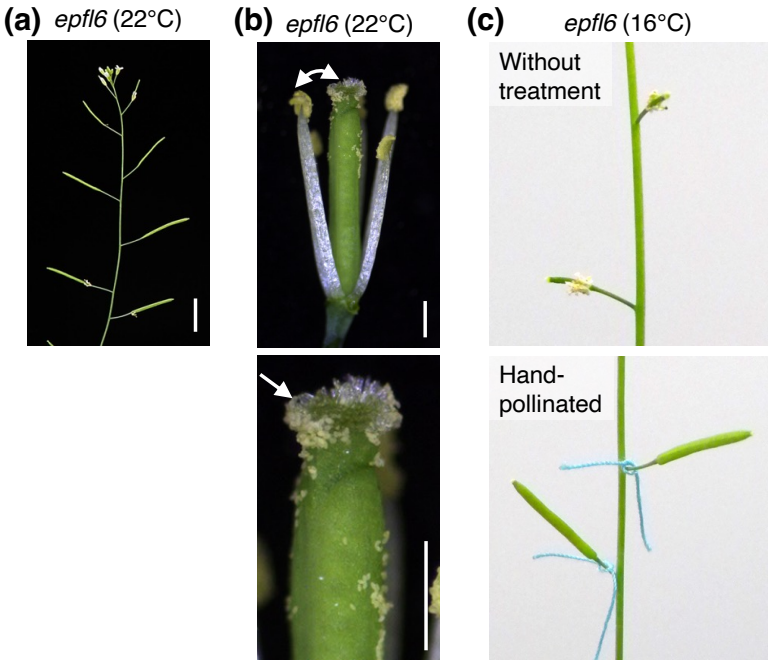

Figure S1

Effects of *epfl4* and *epfl6* single mutations on successful self-pollination at 16 °C and 22 °C.

(a) Inflorescence of epfl6 at 22 °C. Scale bar, 1 cm. **(b)** Flowers with an about 2.5 mm pistil are shown. Sepals and petals were removed to observe stamens and a pistil of each flower. Lower panels show enlarged images near the stamen tip. Double-headed arrows indicate successful pollination between stamens and the pistil of the nearly same length. Arrows indicated pollen attachment to the stigma or the pistil's side position apart from the stigma. Scale bar, 0.5 mm. **(c)** *epfl6* plants grown at 16 °C do not develop siliques due to the failure of self-pollination (upper). However, when a pistil was artificially pollinated with pollens from stamens in the same flower, the pistil develops into a functional silique even at 16 °C (lower). The treated pistils were marked with blue thread.

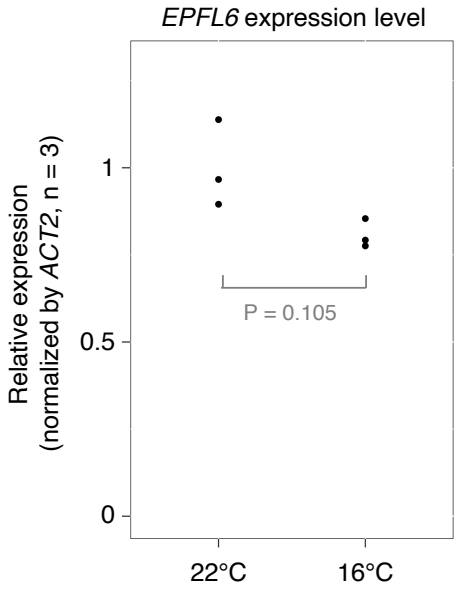

Figure S2

***EPFL6* expression levels in filaments at 16 °C and 22 °C.**

Expression levels of *EPFL6* in wild-type filaments at 22 °C and 16°C measured by quantitative reverse transcription PCR (qRT-PCR). Expression levels with three biological replicates were normalized with respect to that of *ACT2* and the average value of 22 °C was set at 1. Filaments after the removal of anthers were used for RNA extraction. 42 filaments were collected as a pool for each sample. P-value was determined by a Welch's t-test (two-tailed).

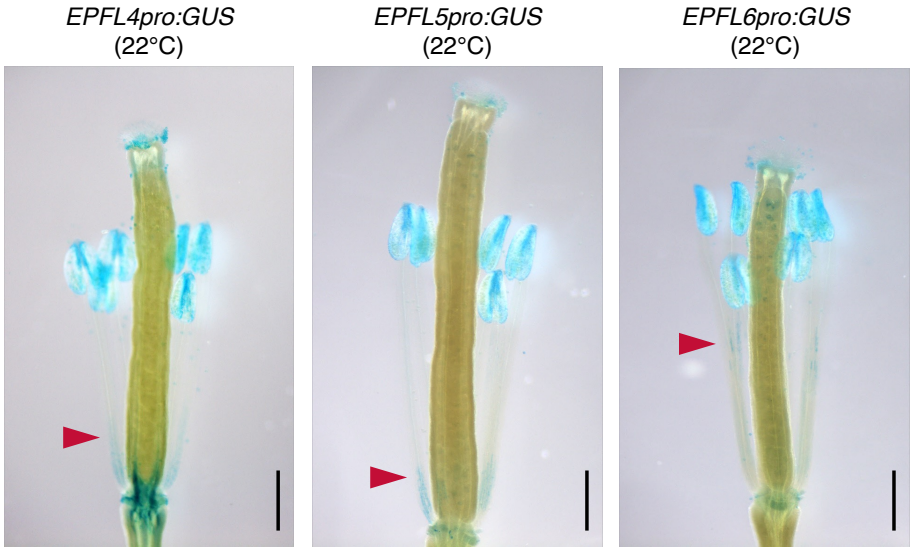

Figure S3

***EPFL4*, *EPFL5* and *EPFL6* are expressed in filaments.**

GUS-stained flowers from plants grown at 22 °C. Sepals and petals were removed from cleared samples to observe stamens and a pistil. Red arrowheads indicate GUS signals in stamen filaments. Scale bar, 0.5 mm.

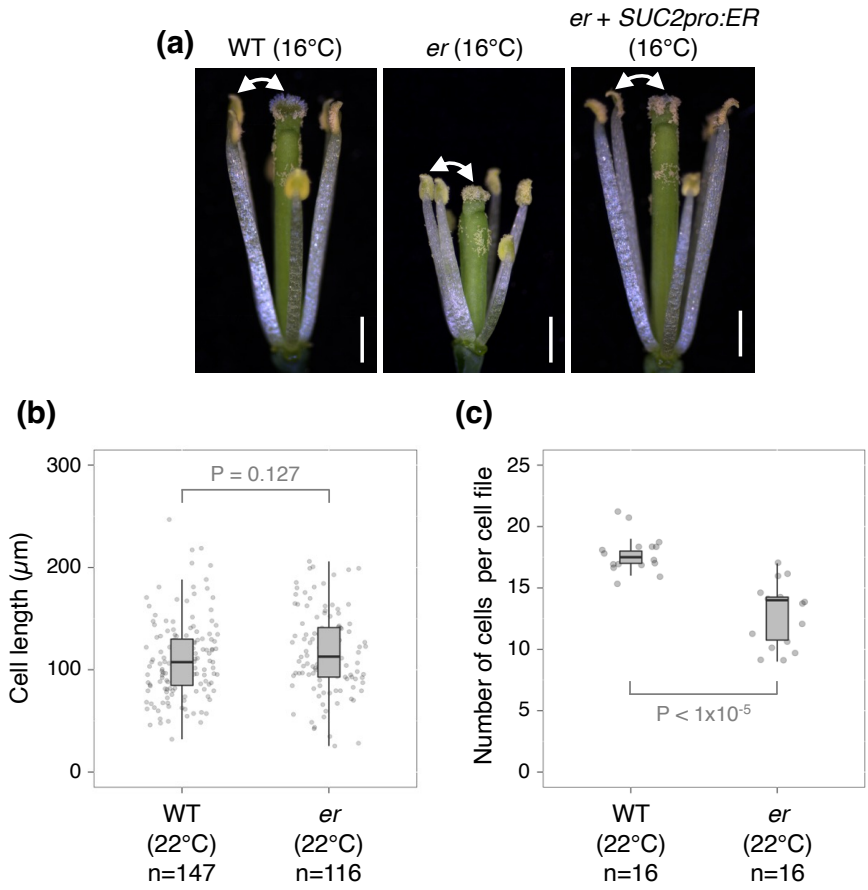

Figure S4

Effects of *er* mutation on successful self-pollination at 16 °C and the length and number of filament cells at 22 °C.

(a) Flowers at the developmental stage suitable for self-pollination. Sepals and petals were removed to observe stamens and a pistil of each flower. The double-headed arrows indicate successful pollination between stamens and the pistil of the nearly same length. Scale bar, 0.5 mm. **(b)** Length of cells in the epidermis of mature filaments. Cell length along the long axis of the filament was measured using eight filaments from four flowers (two long stamens were randomly chosen per flower). Dots indicate the length of each cell. Box-and-whisker plots show a median (centerline), upper/lower quartiles (box limits), and maximum/minimum except for outliers (upper/lower whiskers). P-values were determined by a Welch's t-test (two-tailed). **(c)** Number of cells per cell file of the epidermis of mature filaments. Cells from the bottom end to the top end of each file were counted using sixteen files from four flowers (four long stamens per flower). Dots indicate the number of cells included in each file. Box-and-whisker plots show a median (centerline), upper/lower quartiles (box limits), and maximum/minimum except for outliers (upper/lower whiskers). P-values were determined by a Welch's t-test (two-tailed).

Table S1

List of plasmids constructed in this study

Plasmid	Bacteria selection	Plant selection
SCRpro:GUS:NOSt in pBI101	Kan	Kan
IAA19pro:GUS:NOSt in pBI101	Kan	Kan
EPFL6pro:EPFL6:EPFL6t in pBIN30	Kan	BASTA
SCRpro:EPFL6:NOSt in pBIN30	Kan	BASTA
IAA19pro:EPFL6:NOSt in pBIN30	Kan	BASTA

Table S2

List of primers used in this study

Primer name	Sequence	Purpose
gEPFL6-F2-AscI	TTGGCGCGCCGTAATACAACAATGATTTAGTACCACTAG	*EPFL6* genomic fragment for *EPFL6pro:EPFL6*
gEPFL6-R2-AscI	TTGGCGCGCCGCAGACTAATTATTTCTCTATTGTTTGATCTG	*EPFL6* genomic fragment for *EPFL6pro:EPFL6*
EPFL6-BamHI-F	CGGGATCCGTAATTATGGGTTTCGAGAGAACATC	*EPFL6* coding sequence for *SCRpro/IAA19pro:EPFL6*
EPFL6-SacI-R	TACCGAGCTCAGATCATGGCATGTACAACTTGTTG	*EPFL6* coding sequence for *SCRpro/IAA19pro:EPFL6*
SCR-pro-F-SalI	CAACGTCGACTGCCAATCTGCGTTCGAAATTC	*SCR* promoter for *SCRpro:GUS/EPFL6*
SCR-pro-R-SalI	CAACGTCGACGGAGATTGAAGGGTTGTTGGTC	*SCR* promoter for *SCRpro:GUS*
SCR-pro-R-BamHI	CGGGATCCGGAGATTGAAGGGTTGTTGGTC	*SCR* promoter for *SCRpro:EPFL6*
IAA19-pro-F-SalI	CAACGTCGACTAATATTTTATTAACTAACCGAAAACATAAGCAAGAGAATC	*IAA19* promoter for *IAA19pro:GUS/EPFL6*
IAA19-pro-R-BamHI	CGGGATCCTTCTTGAACTTCTTTTTTTCCTCTCACAATTTG	*IAA19* promoter for *IAA19pro:GUS/EPFL6*
ACTIN2-F	TAACAGGGAGAAGATGACTCAGATCA	*ACT2* qRT-PCR
ACTIN2-R	AAGATCAAGACGAAGGATAGCATGAG	*ACT2* qRT-PCR
EPFL6-L	CCTGCCTTGCTTACGATCTC	*EPFL6* qRT-PCR
EPFL6-R	CCGATCTTCCTAGTCTTCTTTATCAC	*EPFL6* qRT-PCR